American Journal of Emergency Medicine 72 (2023) 72–84

Contents lists available at ScienceDirect

American Journal of Emergency Medicine

journal homepage: www.elsevier.com/locate/ajem

What echocardiographic findings differentiate acute pulmonary embolism and chronic pulmonary hypertension?

Stephen Alerhand, MD [a,*], Robert James Adrian, MD [b]

[a] Department of Emergency Medicine, Rutgers New Jersey Medical School, 150 Bergen Street, Newark, NJ 07103, USA
[b] Department of Emergency Medicine, Harvard Medical School, 55 Fruit Street, Boston, MA 02114, USA

ARTICLE INFO

Article history:
Received 8 May 2023
Received in revised form 5 July 2023
Accepted 6 July 2023
Available online xxxx

Keywords:
Right ventricular dysfunction
right ventricular strain
right ventricle
echocardiography
point-of-care ultrasound
POCUS
cardiac POCUS
ultrasound
pulmonary embolism
pulmonary hypertension
cor pulmonale
right heart thrombus
clot in transit
right ventricular free wall thickness
tricuspid regurgitation
tricuspid regurgitation pressure gradient
pulmonary artery systolic pressure
pulmonary artery acceleration time
60/60 sign
pulmonary artery early-systolic notching
pulmonary artery mid-systolic notching
McConnell's sign

ABSTRACT

Background: Pulmonary embolism (PE) and pulmonary hypertension (PH) are potentially fatal disease states. Early diagnosis and goal-directed management improve outcomes and survival. Both conditions share several echocardiographic findings of right ventricular dysfunction. This can inadvertently lead to incorrect diagnosis, inappropriate and potentially harmful management, and delay in time-sensitive therapies. Fortunately, bedside echocardiography imparts a few critical distinctions.

Objective: This narrative review describes eight physiologically interdependent echocardiographic parameters that help distinguish acute PE and chronic PH. The manuscript details each finding along with associated pathophysiology and summarization of the literature evaluating diagnostic utility. This guide then provides pearls and pitfalls with high-quality media for the bedside evaluation.

Discussion: The echocardiographic parameters suggesting acute or chronic right ventricular dysfunction (best used in combination) are: 1. Right heart thrombus (acute PE) 2. Right ventricular free wall thickness (acute ≤ 5 mm, chronic > 5 mm) 3. Tricuspid regurgitation pressure gradient (acute ≤ 46 mmHg, chronic > 46 mmHg, corresponding to tricuspid regurgitation maximal velocity ≤ 3.4 m/sec and > 3.4 m/sec, respectively) 4. Pulmonary artery acceleration time (acute ≤ 60-80 msec, chronic < 105 msec) 5. 60/60 sign (acute) 6. Pulmonary artery early-systolic notching (proximally-located, higher-risk PE) 7. McConnell's sign (acute) 8. Right atrial enlargement (equal to left atrial size suggests acute, greater than left atrial size suggests chronic).

Conclusions: Emergency physicians must appreciate the echocardiographic findings and associated pathophysiology that help distinguish acute and chronic right ventricular dysfunction. In the proper clinical context, these findings can point towards PE or PH, thereby leading to earlier goal-directed management.

© 2023 Elsevier Inc. All rights reserved.

1. Introduction

Pulmonary embolism (PE) and pulmonary hypertension (PH) (arising from various etiologies [1]) are potentially fatal disease states encountered in the emergency department. Early diagnosis and timely management improve patient outcomes and survival. In the proper clinical context, echocardiographic findings of acute right ventricular dysfunction [2] can point toward the diagnosis of PE and expedite definitive imaging (i.e. computed tomography pulmonary angiography [CTPA]). For a hemodynamically unstable patient or when CTPA is delayed or unavailable, these findings may prompt administration of anticoagulation or thrombolytics. Alternatively, echocardiographic findings suggestive of chronic right ventricular dysfunction can point toward the diagnosis of PH, whose recognition is critical for appropriate resuscitation. Though PH is formally diagnosed by right heart catheterization (RHC), echocardiography is recommended as the first-line, non-invasive diagnostic test by 2022 European Society of Cardiology (ESC) and European Respiratory Society (ERS) guidelines [3].

Similar echocardiographic findings appear with both acute and chronic right ventricular dysfunction. This can inadvertently lead to incorrect diagnosis, inappropriate and potentially harmful management, and delay in time-sensitive therapies. Fortunately, a few critical

* Corresponding author.
E-mail address: Stephen.Alerhand@gmail.com (S. Alerhand).

https://doi.org/10.1016/j.ajem.2023.07.011
0735-6757/© 2023 Elsevier Inc. All rights reserved.

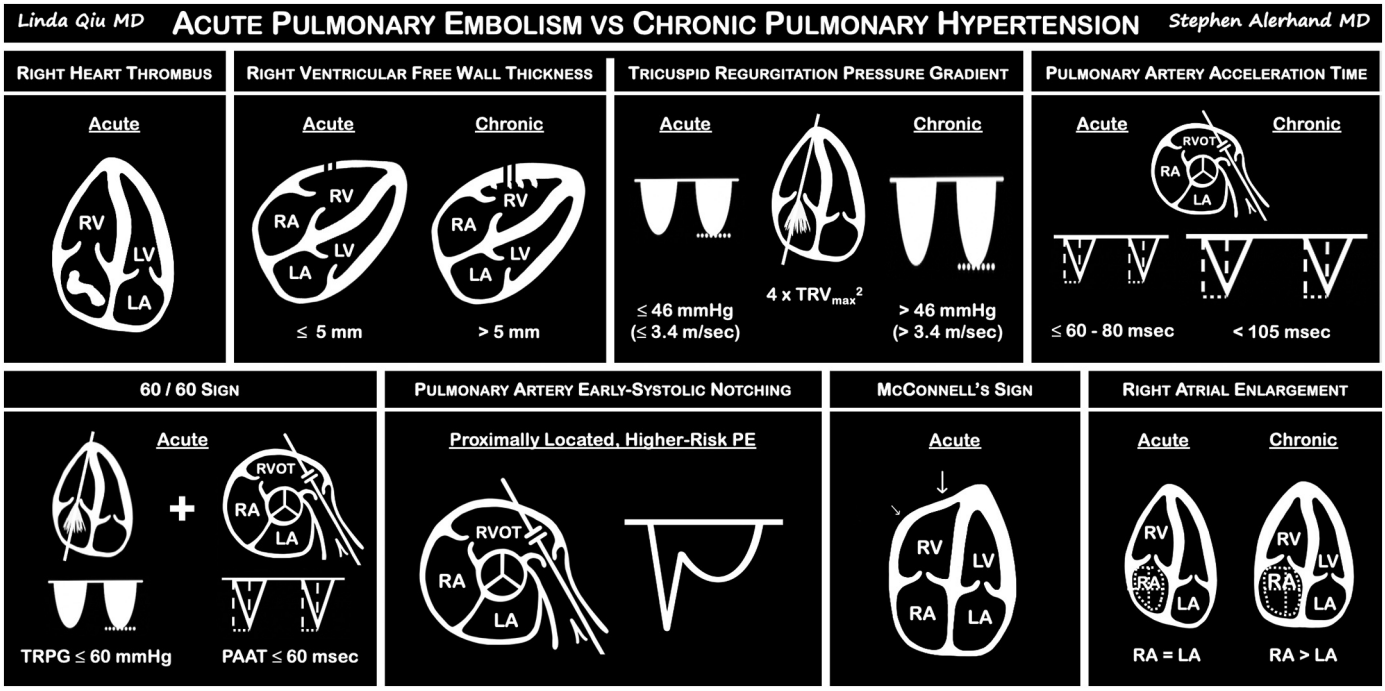

Image 1. Summary Infographic for Distinguishing Acute Pulmonary Embolism and Chronic Pulmonary Hypertension

echocardiographic distinctions between the two disease states can facilitate the correct diagnosis and guide appropriate goal-directed care (Image 1). Combination of these physiologically interdependent variables provides more information than does a single measurement. Emergency physicians should recognize and appreciate these findings.

2. Methods

The authors searched PubMed and Google Scholar for articles using a combination of keywords and MeSH terms “right ventricular dysfunction”, “right ventricular strain”, "right ventricle", “"echocardiography", "point-of-care ultrasound", "POCUS", "cardiac POCUS", pulmonary embolism”, “pulmonary hypertension”, “cor pulmonale”, and each of the echocardiographic parameters listed in the manuscript subheadings. Literature search was restricted to English-language studies. By independent analysis followed by consensus, authors decided which studies to include based on inclusion of pathophysiology, reference cut-off values, or data for a given echocardiographic parameter. When available, societal guidelines and systematic reviews and meta-analyses (SRMAs) were preferentially selected. These were followed by randomized controlled trials, prospective studies, retrospective studies, and reviews. Authors also reviewed supporting citations of included articles. Summative ranges reported in the Evidence subsections were derived from minimum and maximum values obtained from the literature. Unless explicitly stated, values for each echocardiographic parameter did not trend widely in either direction within the range.

3. Discussion

3.1. *RIGHT HEART THROMBUS*

Pathognomonic for acute PE

3.1.1. Description and Pathophysiology

A thrombus from the deep venous system passes through the right atrium (RA) and right ventricle (RV) en route to the pulmonary arterial system. A right heart thrombus (RHT), also known as a clot in-transit, refers to when it lingers temporarily or lodges in the right-sided chambers. Using echocardiography, a RHT appears as a long, thin, free-floating, worm-like mass [4] (Image 2a) (Video 1a). It may intermittently prolapse through the tricuspid valve (TV) or pulmonic valve (PV) during the cardiac cycle. Whether or not there is pre-existing chronic right ventricular dysfunction, presence of a RHT suggests another thrombus (i.e. a PE) is already lodged in the pulmonary arterial system causing acute right ventricular dysfunction. Of the echocardiographic parameters described in this manuscript, a RHT is the sole clear indicator for distinguishing acute-on-chronic from chronic right ventricular dysfunction.

3.1.2. Evidence

SRMAs in 2007 and 2022 reported that a RHT was 4.7-5% sensitive and 99-100% specific for PE [5,6]. Among several large patient registries and SRMAs, prevalence of RHT in patients with PE has ranged from 1.8-8.7% [7-12]. Prevalence reaches up to 16-19% in patients who are hemodynamically unstable [10,13] or in the intensive care unit (ICU) [14]. Factors associated with a RHT in PE include congestive heart failure (CHF), cancer, immobilization, recent major bleeding, and a pre-existing central venous catheter [7,9,11].

3.1.3. How to Assess

Look for a RHT in echocardiographic views in which the right-sided chambers are well-visualized: right ventricular inflow (RVI), parasternal short-axis (PSAX) (at aortic valve [AV] level), apical 4-chamber (A4C), and subxiphoid (SX) views.

3.1.4. Pearls and Pitfalls

From a clinical perspective, a RHT must be differentiated from a valvular vegetation or cardiac tumor. Similar to a RHT, a vegetation has an irregular, lobulated, or amorphous shape with high-frequency oscillating movement [15-18] (Image 2b) (Video 1b). However, instead of floating freely within the right-sided chambers, a vegetation attaches to the proximal, lower-pressure side of the valve (i.e. in the path of the associated high-velocity regurgitant jet) or to implanted prosthetic material—though it oscillates independently of these structures.

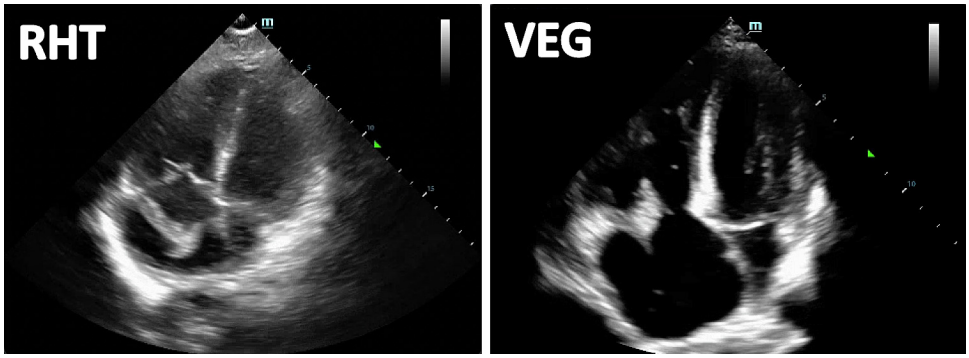

Image 2. Right heart thrombus. A) This RHT appears as a long, thin, free-floating worm-like mass in the RA that intermittently prolapses through the TV during the cardiac cycle. B) This irregularly-shaped, amorphous vegetation is attached to the proximal, lower-pressure side of the anterior TV leaflet and interferes with valvular coaptation. This particular vegetation adheres along a larger surface area of the leaflet and therefore moves more in concert with the leaflet than what is typical (i.e. higher-frequency, independent movement).

Like vegetations, cardiac tumors also have attachment sites, whether to valvular leaflets or chamber walls [17,19,20]. When adhered to the latter, the attachments are more broad-based and infiltrative with local invasion. Tumors may also be associated with a pericardial effusion or vascularity using color Doppler. Other RHT mimics include anatomical RA variants, such as incomplete regression of the Eustachian valve or Chiari network formation from incomplete resorption of the sinus venosus [21].

3.2. *RIGHT VENTRICULAR FREE WALL THICKNESS*

≤ 5 mm suggests acute right ventricular dysfunction
> 5 mm suggests chronic right ventricular dysfunction

3.2.1. Description and Pathophysiology

Normally, the RV carries mass less than ⅙ and diameter less than ⅓ that of the left ventricle (LV) [22,23]. Its free wall is thin and relatively compliant (Image 3a) (Video 2a). Since the pulmonary circulation operates at lower pressure than the systemic circulation, the RV nonetheless ejects the same amount of blood per cycle as the LV, albeit at ⅕ the energy cost [24,25]. Perfusion to the RV by the right coronary artery (RCA) occurs during both diastole and systole [26].

An acute insult such as a PE produces a sudden increase in afterload and vasoconstriction-mediated pulmonary vascular resistance (PVR). The compliant right ventricular free wall immediately bulges outward, causing enlargement of the right ventricular cavity. The increase in wall tension described by the law of LaPlace (∝ ventricular pressure x radius/[2 x wall thickness]) raises myocardial oxygen demand while decreasing right ventricular perfusion [27]. Oxygen consumption also increases from elevated afterload prolonging the isovolumic contraction phase and ejection time. This pathophysiology leads to right ventricular ischemia and further dilation. In this acute setting, the right ventricular free wall has not had time to develop hypertrophy as an adaptation towards reducing wall tension (Image 3b) (Video 2b).

In contrast, with a chronic process such as PH, there is a progressive increase in PVR and decrease in pulmonary vascular compliance. The pulmonary vascular bed no longer allows "storage" of pulmonary blood flow, but rather transitions from a normal high-capacitance state to that of arterial vasoconstriction and proliferative vascular remodeling [28]. The RV initially compensates with increased systolic contraction up to 5-fold to maintain normal stroke volume [29]. This is followed by adaptive hypertrophy that serves to reduce wall tension (Image 3c) (Video 2c). The free wall hypertrophies first [30], followed by the apex and papillary muscles [22,30]. The moderator band traversing the RV near its apex may also hypertrophy [22,31]. Sustained pressure loading eventually leads to right ventricular dilation [32-34]. Moreover, increases in right ventricular afterload and muscle mass are associated with reduction in RCA flow during systole [26,35]. This occurs because compression of myocardial fibers decreases diameter of the microvascular bed and thereby increases vascular resistance. Most RCA flow now occurs only during diastole [26,35]. If right ventricular pressure exceeds systemic blood pressure, further right ventricular ischemia and failure ensue [26,35].

In the normal heart, the RV's free wall (excluding trabeculations) measures 3–5 mm thick in diastole [36]. American Society of Echocardiography (ASE) guidelines posit that right ventricular free wall thickness (RVFWT) > 5 mm in end-diastole using subxiphoid long-axis (SXLA) or parasternal long-axis (PLAX) views indicates right ventricular hypertrophy (RVH), and suggests chronic right ventricular pressure overload in the absence of other pathologies [37].

3.2.2. Evidence

In normal patients, RVFWT has ranged from 3.3-4.0 mm (SXLA) [38-43] and 2.4-4.7 mm (PLAX) [39,41,43-47].

For acute right ventricular dysfunction, 211 ICU patients with PE had RVFWT of 1.7 mm (SXLA) [48].

For chronic right ventricular dysfunction, RVFWT has ranged from 5.6-11.0 mm (SXLA or PLAX) [38,40,42,43,45,46,49-53]. RVFWT ≥ 5 mm (SXLA or PLAX) in patients with various cardiopulmonary conditions has been 90-93% sensitive and 94-95% specific for RVH, as compared to the necropsy reference standard [43,45,46].

3.2.3. How to Assess (Image 3)

1. Acquire a SXLA (preferred) or PLAX view.
2. For qualitative assessment, the right ventricular free wall is considered hypertrophied when it appears as thick as the left ventricular free wall (assuming the latter is not thin from ischemia), with muscular trabeculations and a visible moderator band.
3. For quantitative RVFWT, decrease the imaging depth so that the free wall lies in the center of the screen. Align the focal zone here as well. This produces better spatial resolution for precise measurement.
   a. The screen's resolution (i.e. ability to distinguish between two structures) is superior in the axial plane along the sound waves' axis than in the lateral plane. Therefore, the free wall should be oriented horizontally, such that the caliper tool delineates its measurement perpendicularly to the wall (i.e. in axial plane).
   b. Freeze the B-mode image. Use the ultrasound cine loop to capture a frame in end-diastole, when the RV is largest and the relaxed free wall is thinnest. In SXLA and PLAX, this corresponds to when the TV and mitral valve have only just closed, respectively.
   c. Use calipers to measure RVFWT. Exclude trabeculae, papillary muscles, and epicardial fat [37].
      i. In SXLA, this measurement is obtained below the tricuspid annulus (i.e. toward the right ventricular apex) at the same

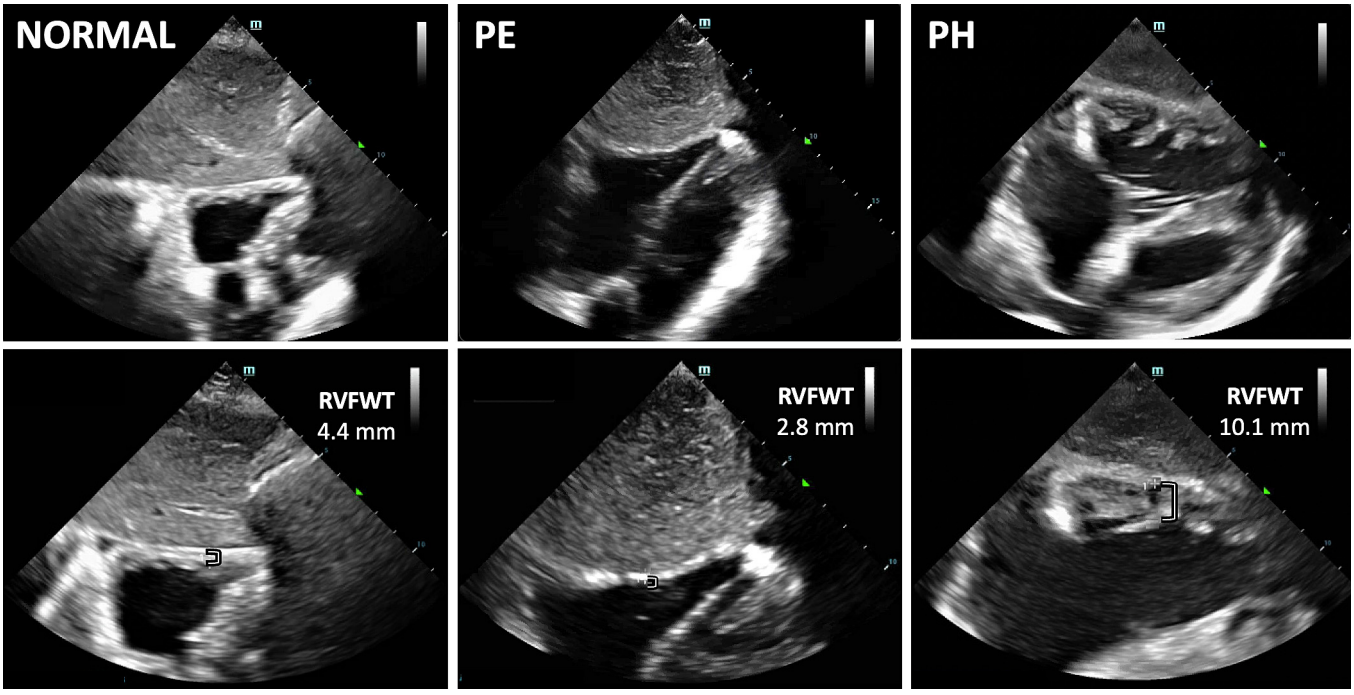

Image 3. Right ventricular free wall thickness. In this normal patient (A) and another with acute right ventricular dysfunction from a PE (B), the right ventricular free wall appears qualitatively thin in comparison to the interventricular septum and left ventricular posterior wall. At decreased depth, the free wall measures ≤ 5 mm thick in end-diastole using the SXLA view. In this patient with chronic right ventricular dysfunction from PH (C), the hypertrophied free wall appears nearly as thick or as thick as the interventricular septum and left ventricular posterior wall, which themselves appear hypertrophied. Thickened trabeculae can also be visualized. At decreased depth, the free wall measures > 5 mm thick.

distance to where the anterior tricuspid leaflet tip would open in diastole [36].

ii. In PLAX, this measurement is obtained at or below the anterior mitral leaflet tip (i.e. towards the left ventricular apex) at a level where the interventricular septum, mitral valve, and posterior left ventricular wall are seen. This position prevents measurements being taken from the right ventricular outflow tract (RVOT).

3.2.4. Pearls and Pitfalls

From a clinical perspective, though endurance athletes are unlikely to present with clinical symptoms suggestive of PH, they may also have increased RVFWT [54,55]. In response to the increase in right ventricular diameter that aims to increase stroke volume, RVH reduces wall stress and increases contractile reserve [56,57]. Nevertheless, this increase in RVFWT is relatively less than that in left ventricular wall thickness [55,57], whereas enlargement of the RV is relatively greater than that of the LV [57]. Per the law of LaPlace, these factors explain why exercise-induced wall stress is larger upon the RV than the LV [56,57].

3.3. TRICUSPID REGURGITATION PRESSURE GRADIENT

≤ 46 mmHg (tricuspid regurgitation maximal velocity ≤ 3.4 m/sec) suggests acute right ventricular dysfunction

> 46 mmHg (tricuspid regurgitation maximal velocity > 3.4 m/sec) suggests chronic right ventricular dysfunction

3.3.1. Description and Pathophysiology

With an acute insult such as a PE, increased PVR leads to dilation and outward ballooning of the thin, compliant right ventricular free wall. The anterior tricuspid leaflet gets pulled outward (beyond the leaflets' 4-9 mm coaptation reserve) [58]. Additionally, tension upon the chordae tendineae causes apical displacement of the tricuspid leaflets [59-61]. Together, these forces lead to decreased (i.e. poorer) valvular coaptation. As a result, blood flow regurgitates through the now rounder (vs. ellipsoid) and flatter (vs. non-planar) TV annulus (Image 4a) (Video 3a) [62]. With chronic pressure overload such as in PH, adaptive RVH occurs over time, followed by ventricular dilation and functional TR through the same mechanism (Image 4b) (Video 3b) [2,61]. This TR results in right ventricular volume overload, which feeds back and causes further annular dilatation, with worsening of that functional TR [61].

The greater the right ventricular pressure pushes against the pulmonary arterial system, the higher the tricuspid regurgitation velocity (TRV) will flow in the retrograde direction. The tricuspid regurgitation pressure gradient (TRPG) is the difference in pressure between RV and RA ($\Delta P_{RV\text{-}RA}$). It is determined by inputting the tricuspid regurgitation maximal velocity (TRV_{max}) into the modified Bernoulli equation ($TRPG = \Delta P_{RV\text{-}RA} = 4 \times TRV^2_{max}$) or allowing automatic calculation by ultrasound machine software [37,63] (Image 5). Per ASE guidelines, normal values for TRV_{max} are ≤ 2.8-2.9 m/sec (TRPG ≤ 31.4-33.6 mmHg) [37]. Large datasets of patients with normal cardiac structure and function reported a TRPG range of 16.0-18.3 mmHg (TRV_{max} 2.0-2.1 m/sec) [64,65], with only 0.5% demonstrating TRPG > 31.4 mmHg (TRV_{max} > 2.8 m/sec) [65].

With acute right ventricular dysfunction, the TRPG will likely remain ≤ 46 mmHg (TRV_{max} ≤ 3.4 m/sec) (Image 5a). In contrast, the TRPG likely only exceeds 46 mmHg (and more so, 60 mmHg [TRV_{max} > 3.9 m/sec]) with chronic dysfunction (Image 5b). As opposed to the thin, non-hypertrophied RV in the setting of an acute PE, the RV's adaptive hypertrophy over time allows it to produce such elevated pulmonary pressures [50,66]. Of note, the value of 46 mmHg is not intended as a strict cut-off marker, but rather a reasonable estimate along the spectrum from acute to chronic right ventricular dysfunction. It derives from 2022 ESC guidelines positing that a TRPG > 46 mmHg (TRV_{max} >3.4 m/sec) suggests high probability of PH being present [3]. An alternate consideration for our proposed TRPG "cut-off value" was ≤ 60 mmHg (TRV_{max} ≤ 3.9 m/sec), as used for the 60/60 sign [67,68]. However, based on available evidence, this higher "cut-off value" would too often attribute chronic right ventricular dysfunction to an acute insult (e.g. when TRPG 47-59 mmHg).

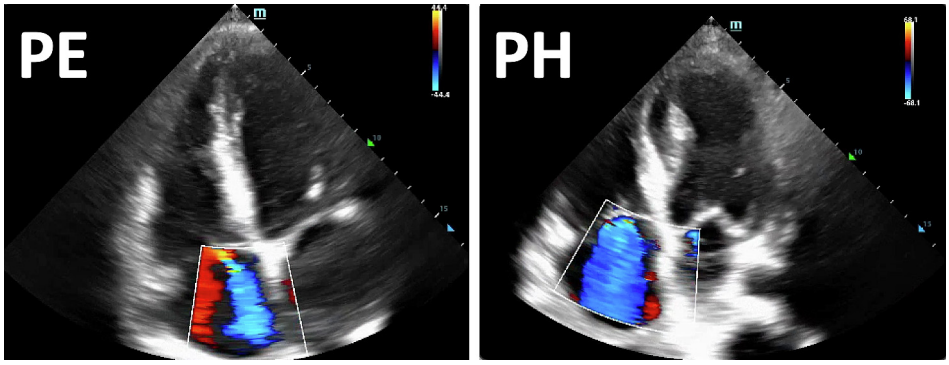

Image 4. Tricuspid regurgitation using color Doppler. A) *TR in acute right ventricular dysfunction from a PE.* In this A4C view, the central jet reflects moderate TR due to the following: encompasses < 50% of the RA, has vena contracta between 3-6.9 mm (which reflects the cross-sectional area of blood leaving the regurgitant orifice), reaches the superior (i.e. back) wall of the RA, and is not holosystolic. The RA appears as large as the LA. B) *TR in chronic right ventricular dysfunction from PH.* In this A4C view, the central jet encompasses > 50% of the RA, has wide vena contracta ≥ 7 mm, reaches the superior wall of the RA, and is holosystolic. The RA appears larger than the LA, with interatrial septal bowing.

ASE guidelines prefer using pulmonary artery systolic pressure (PASP) instead of TRPG to evaluate for right ventricular dysfunction [37]. PASP is obtained by adding the estimated right atrial pressure (RAP) to the TRPG (i.e. PASP = $4 \times TRV_{max}^2 + RAP$). In contrast, 2022 ESC/ERS and British Society of Echocardiography (BSE) guidelines prefer using TRPG, while omitting RAP due to inaccuracies in its estimation from inferior vena cava (IVC) diameter and respirophasic collapsibility [3,69]. A 2016 systematic review found most studies demonstrated only moderate-strength correlations between IVC diameter and RAP [70]. One study found that RAP estimation performed well for low or high RAP, but worse for intermediate values [71]. Moreover, evidence for user reliability in emergency physicians assessing IVC diameter is mixed (and often suboptimal) [72-75]. Furthermore, rather than provide a precise value for RAP, ASE guidelines only offer discrete estimates of 3, 8, or 15 mmHg (corresponding to thin/collapsible IVC, in-between, and dilated/non-collapsible, respectively) [37]. At a PASP roughly close to the acute-vs-chronic "cut-off value" (as opposed to being sufficiently low or high), lack of a more precise RAP estimate would complicate distinction between the two disease entities solely based on PASP. Lastly, the ASE's maximal designation of 15 mmHg may underestimate RAP in severe PH, when actual RAP may exceed 30 mmHg [76]. Therefore, for helping to differentiate between acute and chronic right ventricular dysfunction, we suggest using TRPG rather than PASP.

3.3.2. Evidence

For acute right ventricular dysfunction, patients with PE having detectable TR by color Doppler have demonstrated higher TRPG values than those without PE (21.1-49.0 vs. 10.2-28.0 mmHg, TRV_{max} 2.3-3.5 vs. 1.6-2.6 m/sec) [10,48,67,68,77-84]. TRPG values have ranged higher with proximally-located, higher-risk PEs than with lower-risk PEs (38.4-49.2 vs. 31.4-38.4 mmHg, TRV_{max} 3.1-3.5 vs. 2.8-3.1 m/sec) [10,82-84].

For chronic right ventricular dysfunction, the TRPG in patients with PH having detectable TR has ranged from 52.0-92.0 mmHg (TRV_{max} 3.6-4.8 m/sec) [49,50,61,68,85-93].

In one study comparing acute to chronic right ventricular dysfunction, the TRPG was lower in those patients with acute PE than in those with chronic proximal PE, chronic parenchymal lung disease, and primary PH (48 vs. 79, 55, and 92 mmHg, respectively; TRV_{max} 3.5 vs. 4.4, 3.7, and 4.8 m/sec, respectively) [68].

3.3.3. How to Assess (Image 5)

1. Assess for TR using color Doppler in the RVI, PSAX (at AV level), A4C (Image 4) (Video 3), SXLA, and subxiphoid short-axis (SXSA) (at AV level) views.
   a. In these views, the transmitter's emitted sound waves are oriented roughly parallel (i.e. 0° angle) to TR flow, which produces the maximal shift in Doppler frequency (cos 0°=1).
   b. Obtaining multiple views increases likelihood of both capturing a TR jet if present and obtaining the maximal TRV.
   c. For highest frame rate and image resolution, imaging depth should be decreased to the minimum required for visualization of the TV and RA. The color Doppler box should only encompass those structures.

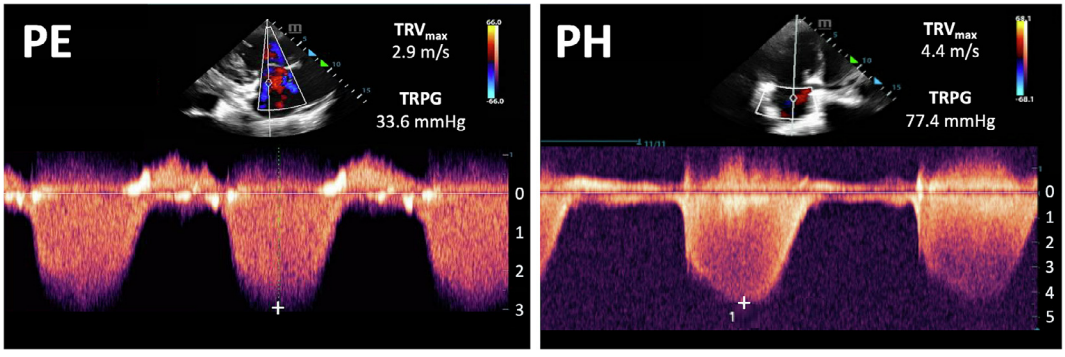

Image 5. Tricuspid regurgitation pressure gradient using continuous wave Doppler. A) *TRPG ≤ 46 mmHg (TRV_{max} ≤ 3.4 m/sec) in acute right ventricular dysfunction from a PE.* Without Doppler angle correction, the highest TRV_{max} was obtained from the RVI view. The waveform is dense (vs. faint), which reflects a large number of red blood cells traveling at those velocities. The shape appears parabolic, which implies a steady rise and fall in regurgitant blood velocity. These findings together suggest moderate TR. B) *TRPG > 46 mmHg (TRV_{max} > 3.4 m/sec) in chronic right ventricular dysfunction from PH.* Without Doppler angle correction, the highest TRV_{max} was obtained from the A4C view. The waveform is dense. The shape appears parabolic, and less triangular than would be expected if there were earlier equalization of right ventricular and right atrial pressures during systole (i.e. having early velocity peak and rapid deceleration)—perhaps due to the markedly enlarged RA. These findings together suggest severe TR. Of note, this waveform's amplitude appears grossly similar on the imaging screen as that of A), but this is because the scale on the y-axis goes up to 5 m/sec versus only 3 m/sec for A).

2. Align the continuous wave Doppler (CWD) beam in same direction as the TR jet. Place the beam focus within center of the jet. CWD allows recording of higher velocities than pulsed wave Doppler (PWD) and can thus avoid aliasing.
   a. To avoid underestimation of Doppler frequency, the angle $\boldsymbol{\theta}$ between CWD beam and TR flow should ideally be 0° (i.e. parallel to one another) but is recommended to lie within 20°.
      i. With errors of 10° and 20°, the Doppler shift is only underestimated by 2% and 6%, respectively [63]. With errors of 30° and 45°, the Doppler shift is underestimated by 13% and 29%, respectively. These percent errors are amplified in the modified Bernoulli equation because TRV_{max} is squared.

3. Press the CWD button again. The TRV spectral waveform appears as a downward deflection on the y-axis.
   a. Use sufficiently high sweep speed (~100 mm/sec) to stretch out the waveforms and thereby better discriminate true velocities from sonographic artifacts.
   b. Adjust the y-axis scale and baseline so that the waveform takes up as much of the screen as possible without aliasing. This provides for the most precise velocity determinations.
   c. To avoid overestimation of TRV_{max}, decrease Doppler gain to minimize spectral noise.

4. Freeze the frame. Place the cursor at the outer edge of the largest trough to obtain TRV_{max} from that particular echocardiographic view.
   a. Avoid obtaining velocities from non-representative beats, which may occur immediately following premature ventricular contractions. For patients with atrial fibrillation, use the third beat after two consecutive equally-spaced heartbeats, or take the average from at least five heartbeats [94].
   b. Record TRV_{max} only for well-defined, dense, spectral profiles.

5. Enter TRV_{max} into the modified Bernoulli equation ($TRPG = 4 \times TRV_{max}^2$) or employ the machine software's automatic calculation.

3.3.4. Pearls and Pitfalls

From a clinical perspective, normal patients that do have detectable TR using color Doppler will have a TRPG ≤ 46 mmHg ($TRV_{max} < 3.4$ m/sec), just as with acute PE. Therefore, use of TRPG to differentiate between acute and chronic right ventricular dysfunction should only be applied when these medical conditions are suspected. Secondly, TRPG depends not only on resistance of the pulmonary circulation, but also on pulmonary flow and left atrial pressure [76]. For example, high-output (e.g. pregnancy, anemia) or high-volume states (e.g. pulmonary edema), or those with increased pulmonary venous and left atrial pressures (e.g. CHF or mitral valvulopathies), may show an elevated TRPG despite low PVR [95]. Moreover, hypoxia from acute respiratory illness leads to pulmonary vasoconstriction and increased PVR, which also increases TRPG [96].

Third, in severe right ventricular failure, there may not be sufficient systolic force to generate a TR jet. Any measurable TRPG will not reflect severity of right ventricular dysfunction even if PVR is high [95,97]. Fourth, with severe TR, earlier equalization of right ventricular and atrial pressures in systole results in rapid deceleration of the spectral waveform, which leads to underestimation of TRPG [36,98-101]. In case of a wide-open tricuspid annulus, free and broad TR flow causes the right heart to essentially act as a single chamber during systole [102]. The modified Bernoulli equation only applies for narrow orifices with steady laminar flow, and not when the inertial component of the equation must be incorporated [103]. The equation assumes complete conversion of potential energy (i.e. high pressure in the RV) into kinetic energy (i.e. high-pressure TR jet), so TRPG obtained in these cases does not represent the true severity of right ventricular dysfunction.

Fifth, data from 3,790 patients with normal cardiac structure and function suggests the upper limit of normal TRPG may reach up to 30 mmHg (TRV_{max} 2.7 m/sec) in patients > 50 years-old (from decreased pulmonary artery [PA] compliance or increased left ventricular diastolic pressure) or with body mass index > 30 kg/m^2 [64].

From a technical perspective, an eccentric TR jet (i.e. directed toward the RA's medial or lateral wall) will appear smaller using color Doppler than a central jet of equal or lower severity [58,62]. Known as the Coanda effect, this hydrodynamic phenomenon occurs due to loss of the jet's kinetic energy from absorption by the atrial wall. These friction thermal and viscous losses are not accounted for by the modified Bernoulli equation, leading to underestimation of TRPG [104]. Second, the TR Doppler technique cannot be applied in cases of RVOT obstruction or pulmonary stenosis (which is mostly associated with congenital heart disease). In such cases, the TRPG obtained would reflect blood flow trying to pass through the obstructed RVOT or stenotic PV, respectively, and not through the PA as desired.

3.4. *PULMONARY ARTERY ACCELERATION TIME*

≤ 60-80 msec suggests acute right ventricular dysfunction
< 105 msec suggests chronic right ventricular dysfunction

3.4.1. Description and Pathophysiology

On the PA systolic ejection waveform, pulmonary artery acceleration time (PAAT) (also known as RVOT acceleration time) refers to the time interval from onset of PA ejection to peak flow velocity across the PV [105,106] (Image 6a, b, c). Normally, the pulmonary circulation is a low-resistance, high-compliance circuit that can recruit additional vasculature. It allows pulmonary blood to be "stored", thereby facilitating low right ventricular afterload [28]. The waveform demonstrates gradual acceleration, peak velocity in middle of systole, and gradual symmetric deceleration (Image 6a). This dome-like profile occurs due to slow, steady increase and decrease in PA pressure during systole [107,108]. Moreover, the low-resistance pulmonary circulation only reflects back a small retrograde pressure wave, indicative of a low reflection coefficient (i.e. ratio of peak reflected:anterograde pressures) [109]. This slowly-propagating reflected wave does not reach the RVOT until diastole, after the RV has already completed systolic ejection [110-112]. This small, late-arriving retrograde wave only minimally dampens the anterograde wave and contributes to PV closure [112,113]. In a pooled analysis of 1,479 healthy patients, mean PAAT was 138.7 ± 17.5 with a 5% lower quantile of 103.7 msec [106].

The 2022 ESC/ERS and BSE guidelines posit that PAAT < 105 msec increases probability of PH being present [3,69]. PAAT weakly correlates with age, body mass index, systolic and diastolic blood pressures, and diastolic heart function [106]. Its diagnostic capability is not affected by etiology of PH or presence of arrhythmias [105].

With acute right ventricular dysfunction, pressure waves emitted from the RVOT propagate more rapidly in the non-compliant pulmonary arteries [66,67,114,115]. This manifests as a PA systolic ejection waveform with steeper acceleration, earlier peak velocity (thus, a shorter PAAT), and steeper deceleration due to earlier pressure equilibration between RVOT and PA (Image 6b) [108,116]. These changes produce a more triangular (vs. dome-shaped) waveform. Moreover, the higher-resistance pulmonary arterial system reflects a larger retrograde wave (indicative of a higher reflection coefficient) that more rapidly propagates and reaches the RVOT during (vs. after) systole. This wave reflection increases ventricular afterload and dampens the anterograde pressure wave by essentially subtracting from it [109,112-114,117-119]. PAAT in acute right ventricular dysfunction is generally ≤ 60-80 msec. Of note, this value is not intended as a strict cut-off marker, but rather a reasonable estimate along the spectrum from acute to chronic right ventricular dysfunction. An alternate consideration for our proposed "cut-off value" was PAAT ≤ 60 msec, as used for the 60/60 sign [67,68]. However, given the 60/60 sign's potentially

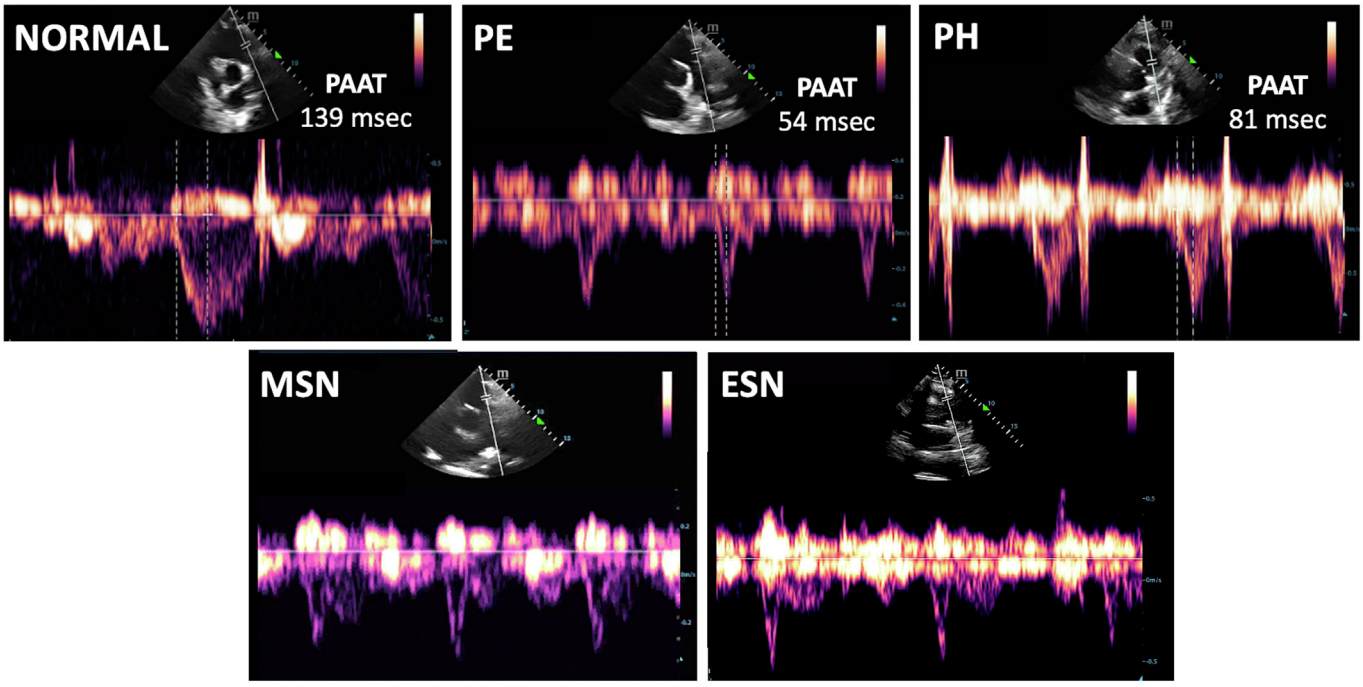

Image 6. Pulmonary artery systolic ejection waveforms. A) PAAT > 105 msec in a normal patient. B) PAAT ≤ 60-80 msec in acute right ventricular dysfunction from a PE. There appears to be early development of a spike-and-dome pattern. C) PAAT < 105 msec in chronic right ventricular dysfunction from PH. D) MSN (i.e. spike-and-dome pattern in second half of the waveform) in acute right ventricular dysfunction from a peripherally-located, lower-risk PE. This pattern can also appear with PH. E) ESN (i.e. in first half of the waveform) from a proximally-located, higher-risk PE.

low sensitivity for PE (13-71%) [10,67,68,82,120,121], that lower "cut-off value" would too often attribute an acute insult to chronic right ventricular function (e.g. when PAAT 61-80 msec). Instead, our "cut-off value" was determined by combination of the 60/60 sign and available evidence (see Section 3.4.2).

For chronic right ventricular dysfunction, PAAT is generally shorter than normal (i.e. < 105 msec) but longer than with an acute process (i.e. ≤ 60-80 msec)—hence 81-104 msec (Image 6c). This occurs because the pulmonary vasculature has had time to develop compliance. The speed of pressure waves emitted from the RVOT, as well as the size (and accordingly, the reflection coefficient) and speed of the reflected retrograde wave, lie in between those values from normal patients (i.e. slowly-propagating anterograde wave; small, slowly-propagating retrograde wave) and those with acute right ventricular dysfunction (i.e. rapidly-propagating anterograde wave; larger, rapidly-propagating retrograde wave). Consequently, the slope of the PA systolic ejection waveform and time to reach peak velocity (i.e. the PAAT) also lie in between those associated with normal patients (i.e. gradual slope, longer time to peak velocity) and those with acute right ventricular dysfunction (i.e. steeper slope, shorter time to peak velocity). Of note, in a patient with other echocardiographic findings indicative of chronic PH, an otherwise-contradictory PAAT ≤ 60-80 msec could suggest acute-on-chronic dysfunction from an acute PE.

3.4.2. Evidence

For acute right ventricular dysfunction, patients with PE have demonstrated shorter PAAT values than those without PE (48-97 vs. 95-162 msec) [10,67,68,79,81,82,84,122-126].

For chronic right ventricular dysfunction, patients with PH have demonstrated shorter PAAT values than those without PH (69-90 vs. 88-143 msec) [85,89,90,93,127-131].

In one study comparing acute to chronic right ventricular dysfunction, PAAT was shorter in those patients with PE than with chronic proximal PE, chronic parenchymal lung disease, and primary PH (56 vs. 59, 69, and 64 msec, respectively) [68].

3.4.3. How to Assess (Image 6a, b, c)

1. Acquire a PSAX or SXSA [132] view at AV level for simultaneous visualization of RVOT, PV, and PA.
   a. For highest frame rate and image resolution, imaging depth should be decreased to the minimum required for visualization of these structures. The focal zone should be focused on the PV. This facilitates PWD sampling from the most precise location.

2. Place the PWD sampling gate in the RVOT 0.5-1.0 cm proximal to the PV's insertion points. Align the beam roughly in the same direction as blood flow.

3. Press the PWD button again. The PA systolic ejection waveform appears as a downward deflection on the y-axis.
   a. By properly placing the sampling gate (i.e. not too distally), the waveform depicts a closing click (from PV closure) but not an opening click (from PV opening).
   b. Increase sweep speed to stretch out the waveforms and allow for better discrimination of time intervals.
   c. Adjust the y-axis scale and baseline so that the waveform takes up as much of the screen as possible without aliasing. This provides for the most precise determination of the waveform's onset and peak.

4. Freeze the frame. Use calipers to measure the time interval on the x-axis from onset of PA systolic ejection to peak velocity (i.e. PAAT).

3.4.4. Pearls and Pitfalls

From a technical perspective, very precise angulation of the PWD beam is not required for obtaining PAAT. Even if the angle between beam and direction of blood flow lies within reasonable deviation from 0°, the shape of the PA systolic ejection waveform will remain the same. Correspondingly, the time interval on the x-axis from onset of PA ejection to peak velocity (i.e. PAAT) will also remain the same.

3.5. 60/60 SIGN

Suggests acute right ventricular dysfunction

3.5.1. Description and Pathophysiology

A TRPG ≤ 60 mmHg (TRV_{max} ≤ 3.9 m/sec) (Image 5a) and PAAT ≤ 60 msec (Image 6b) together comprise the 60/60 sign, which suggests acute right ventricular dysfunction [67,68].

3.5.2. Evidence

For acute right ventricular dysfunction, studies evaluating the 60/60 sign have demonstrated 13—71% sensitivity and 69–98% specificity for PE [6,10,67,68,82,120,121]. Sensitivity is higher with proximally-located, higher-risk PEs than with lower-risk PEs (31-87% vs. 7-44%) [10,82,121].

3.5.3. How to Assess

1. TRPG is obtained by inputting TRV_{max} into the modified Bernoulli equation or employing ultrasound machine software (see Section 3.3.3) (Image 5a).
2. PAAT is obtained from the PA systolic ejection waveform (see Section 3.4.3) (Image 6b).

3.5.4. Pearls and Pitfalls

A common misconception is that the 60/60 sign incorporates PASP ≤ 60 mmHg, rather than TRPG ≤ 60 mmHg as the original studies intended [67,68]. Otherwise, the caveats previously described for TRPG (Section 3.3.4) and PAAT (Section 3.4.4) apply.

3.6. PULMONARY ARTERY EARLY-SYSTOLIC NOTCHING

Suggests a proximally-located, higher-risk PE

3.6.1. Description and Pathophysiology

Once PA pressure reaches a certain threshold, the retrograde wave (see Section 3.4.1) causes transient reversal of the systolic gradient between PA and RVOT. Abrupt reduction in anterograde PA systolic velocity manifests as a biphasic spectral waveform appropriately known as "mid-systolic notching" (MSN) (Image 6d) [68,107,112-115,133-139]. The associated "spike-and-dome" pattern appears as a narrow-peaked waveform (i.e. "spike") with early deceleration toward the notch, followed by a second more-rounded waveform (i.e. "dome") [82]. The notch reflects the subtraction from anterograde wave velocity by reflected wave velocity [114,117].

MSN has been described for evaluating both PE [49,68,82,113,114,128] and PH [107,112,115-117,133,134,136-141]. However, clinical distinction can potentially be made based on the notch's temporal location on the x-axis along the PA systolic ejection waveform. In addition to the retrograde wave's propagation velocity and size (and accordingly, the reflection coefficient), notch location is also determined by the site of impedance (i.e. reflection site) in the pulmonary vascular circuit from where the retrograde wave originates [114,115,142-144]. The distance from site of wave propagation (i.e. RVOT) to reflection site is referred to as the reflection distance.

To begin with, patients with pulmonary venous congestion alone (without elevated PVR) will not demonstrate MSN [115]. These patients have a distally-located reflection site in the pulmonary veins and thus, a longer reflection distance. By the time a reflected wave returns to the RVOT, systolic ejection will already have completed. The reflected wave will not arrive in time to dampen or subtract from the anterograde wave. Alternatively, with pulmonary arterial hypertension, the reflection site is located more proximally (i.e. in the pulmonary arterial circuit). Reflection distance is shorter, and earlier wave reflection may cause notching [114,119,145]. Finally, with proximal vascular obstruction caused by PE, the reflection site is located even closer to the RVOT, and this even-shorter reflection distance may cause earlier notching on the PA systolic ejection waveform [114,119].

Therefore, whereas MSN (i.e. in second half of the waveform) can occur with both proximal PA obstruction (i.e. PE) and peripheral pulmonary obstruction (i.e. PH), "early-systolic notching" (ESN) (i.e. in first half) is more likely in proximally-located, higher-risk PEs (Image 6e) [77,82,121]. This suggests the shape of the PA systolic ejection waveform is determined primarily by presence or absence of proximal thromboemboli more so than the degree of elevated PA pressures [68,110]. The more proximal reflection site is thought to occur due to hypoxia-induced PA vasoconstriction caused by the embolus, rather than by direct reflection off the embolus itself [112,113]. Of note, in a patient with other echocardiographic findings indicative of chronic PH, an otherwise-contradictory ESN could suggest acute-on-chronic dysfunction from an acute PE.

In sum, timing and size of the PA retrograde wave reflection are governed by: 1) wave propagation velocity (dependent on PVR and vascular compliance) 2) reflection coefficient 3) reflection site and distance. The reflection distance can help explain the notching location in proximally-located, higher-risk PEs (i.e. ESN) compared to that in PH or peripherally-located, lower-risk PEs (i.e. MSN).

3.6.2. Evidence

For acute right ventricular dysfunction, ESN has been reported as 34-75% sensitive and 99-100% specific for PE [77,121]. Sensitivity and specificity for proximally-located, higher-risk PEs has been 69-97% and 90-99%, respectively [77,82,84], as compared to 2% and 92% for lower-risk PEs [82].

3.6.3. How to Assess

1. Generate the PA systolic ejection waveform (see Section 3.4.3).
2. Evaluate for presence of ESN.

3.6.4. Pearls and Pitfalls

From a technical perspective, the PV's opening click on the PA systolic ejection waveform (see Section 3.4.3) can be a false-positive for ESN [82].

3.7. MCCONNELL'S SIGN

Suggests acute right ventricular dysfunction

3.7.1. Description and Pathophysiology

McConnell's sign refers to diffuse hypokinesis of the RV with intact (or "spared") apical systolic contraction (Image 7) (Video 4) [146]. Its original authors suggested this sign occurs in acute PE and could help distinguish acute from chronic right ventricular dysfunction [146].

Three mechanisms were proposed for this finding. First, by being tethered to the LV, the thin right ventricular apex gets pulled inward by a contracting (and often hyperdynamic) LV [146]. In contrast, an apex hypertrophied over time (as in PH) is not pulled inward as readily. Second, upon encountering acutely increased afterload from a PE, the RV dilates and adapts toward a spherical shape to distribute wall stress more equally. The greater outward bulging of the mid-right ventricular free wall relative to apex merely gives the appearance of free wall hypokinesis [146]. In contrast, RVH associated with PH limits ease of that outward bulging. Third, increased wall tension from acutely increased right ventricular pressure load and subsequent chamber dilation (i.e. per law of LaPlace) raises the free wall's oxygen demand [27]. Simultaneous reduction in RCA perfusion to the free wall (especially during systole) [26,35] results in its hypokinesis [146]. In contrast, the apex receives perfusion from both the RCA and left anterior descending artery. Thus, the apex remains perfused, and its systolic contraction remains intact.

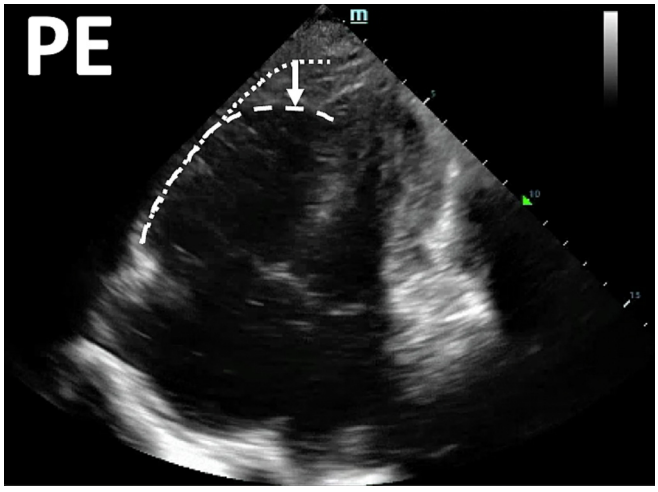

Image 7. McConnell's sign. In this A4C view of a patient with PE, the downward arrow demonstrates the RV's intact apical systolic contraction. This contrasts with absent-to-minimal inward excursion of the mid-free wall. The dotted line delineates what had been the border of the relaxed RV at end-diastole. The dashed line delineates the border at end-systole.

3.7.2. Evidence

SRMAs in 2017 and 2022 reported that McConnell's sign was 22-29% sensitive and 97-99% specific for PE [5,6]. Sensitivity rises with proximally-located, higher-risk PEs [10,82,84,120,147-149].

In one study comparing acute to chronic right ventricular dysfunction, McConnell's sign was found more often in 15 patients with acute PE than in 30 with PH (60% vs. 17%) [150].

3.7.3. How to Assess

1. Acquire an RV-focused A4C view in which the RA and RV are well-visualized.
2. Qualitatively assess for McConnell's sign.

3.7.4. Pearls and Pitfalls

From a clinical perspective, McConnell's sign may also be caused by right ventricular infarction [151-154]. This supports the proposed mechanism that free wall hypokinesis is caused by reduced RCA perfusion.

3.8. *RIGHT ATRIAL ENLARGEMENT*

Equal to left atrial size suggests acute right ventricular dysfunction

Greater than left atrial size suggests chronic right ventricular dysfunction

3.8.1. Description and Pathophysiology

The RA facilitates right ventricular filling via three functions: 1) reservoir - store blood when the TV is closed (i.e. in systole) 2) conduit - receive blood from coronary and systemic veins, and transfer it to the RV when the TV opens (i.e. in early diastole) 3) booster pump (i.e. atrial kick) - contract in late diastole to complete ventricular filling [37,155]. Under normal conditions, a large volume of blood is transferred from RA to RV at low pressure (Image 8a) (Video 5a).

With an acute increase in right ventricular afterload (e.g. PE), functional TR associated with right ventricular dilation leads to right atrial stretching and enlargement (Image 8b) (Video 5b) [51,156]. This compensation for reduced right ventricular contractility increases preload to maintain cardiac output [156,157]. Acutely, there is minimal if any change in right ventricular diastolic function [158,159].

In contrast, development of RVH over time leads to right ventricular diastolic dysfunction through increased wall stiffness and decreased compliance [156]. Passive emptying from RA into RV (i.e. conduit function) thus decreases [160-163]. Elevated diastolic pressure leads to worsening of functional TR and further right atrial enlargement [164] (Image 8c) (Video 5c). To maintain filling of the stiffened RV, right atrial contractility (i.e. booster pump function) increases [51,156,160,163,165,166], as does RAP [167,168]. Eventually, however, right atrial compensation to increase both reserve volume and contractile force reaches its limit. At that point, there is a decrease in cardiac output, and severe right-sided heart failure ensues.

Patients with PE may have a qualitative RA:LA size ratio approaching 1:1 in the A4C or SXLA views, whereas patients with PH usually have size ratio > 1:1 [169-171]. This ratio is not intended as a strict cut-off marker, but rather an evidence-based estimate along the spectrum of acute versus chronic right ventricular dysfunction. ASE guidelines also provide upper reference values for major and minor linear dimensions (> 5.3 cm and > 4.4 cm, respectively), as compared to normal means (4.4 cm and 3.5 cm, respectively) [37]. ASE, ESC/ERS, and BSE guidelines also posit that right atrial area (RAA) > 18 cm^2 indicates chamber enlargement and increases probability of PH [3,37,69], as compared to normal mean of 14 cm^2 [37].

3.8.2. Evidence

For acute right ventricular dysfunction, patients with PE have demonstrated a higher RAA:LAA ratio (0.97-0.98 vs. 0.83) [78,172] and RAA (14.7-18 vs. 13-15 cm^2) [48,78,122,165,173] than those without PE.

For chronic right ventricular dysfunction, the RAA:LAA ratio has been reported as 1.3-1.5 [87,92], and RAA has ranged from 18.0-41.9 cm^2 [49,86,88,125,163,168,174,175].

3.8.3. How to Assess (Image 8)

1. Acquire an RV-focused A4C view in which the RA and RV are well-visualized.
2. Qualitatively assess if the RA appears as large as the LA (as may occur with acute right ventricular dysfunction) or larger (as with chronic right ventricular dysfunction). Also look for interatrial septal bowing into the LA, particularly at end-systole.
3. Use the ultrasound cine loop to obtain a B-mode frame at end-systole just prior to TV opening, when the RA is largest.
4. If quantitative measurements are desired, obtain major (i.e. length) and minor (i.e. diameter) dimensions of the RA, and compare to upper limits of normal (i.e. 5.3 cm and 4.4 cm, respectively).
   a. Major: measure from center of the tricuspid annulus (which extends between insertion points of the anterior and septal leaflets) to center of the superior right atrial wall's inner edge, parallel to the interatrial septum.
   b. Minor: measure from right atrial mid-free wall to interatrial septum (inner-edge to inner-edge), perpendicular to the major dimension.
5. The RAA can also be obtained and compared to upper limit of normal (i.e. 18 cm^2).
   a. Trace the RA's blood-tissue interface along the tricuspid annular plane, interatrial septum, superior wall, and lateral wall.
      i. Exclude the triangular space between tricuspid leaflet tips and tricuspid annulus, as well as the IVC, superior vena cava, and right atrial appendage.

3.8.4. Pearls and Pitfalls

From a technical perspective, accuracy of linear dimensions is limited by measurements arising from only a single dimension [36]. RAA values are limited by assumption of a symmetric cavity shape.

4. Conclusion

The echocardiographic parameters suggesting acute PE or chronic PH (best used in combination) are: 1. Right heart thrombus (acute PE)

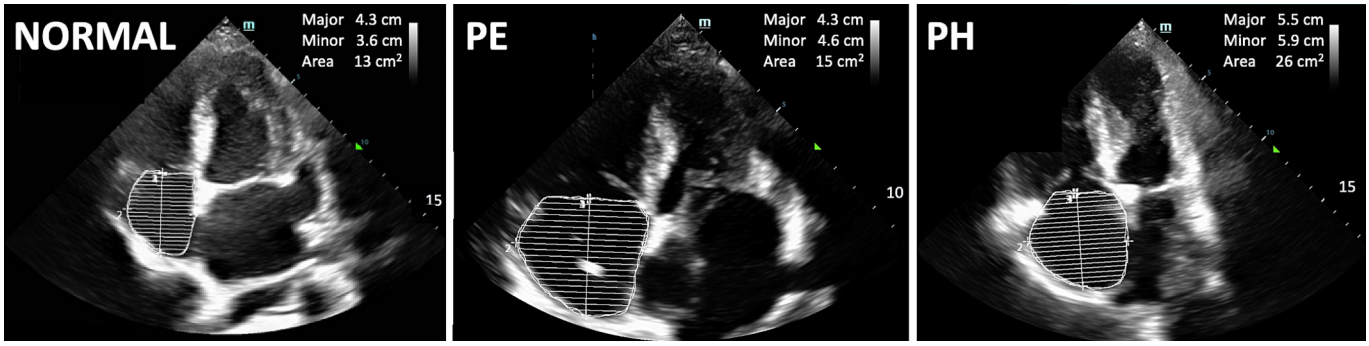

Image 8. Right atrial size. A) In this normal patient, the RA:LA size ratio is < 1:1. Major/minor dimensions and RAA are below upper reference values for normal. B) In this patient with acute right ventricular dysfunction from a PE, the RA:LA size ratio approaches 1:1. The major dimension and RAA remain below upper reference values for normal. C) In this patient with chronic right ventricular dysfunction from PH, the RA:LA size ratio is > 1:1. Major/minor dimensions and RAA are above reference values for normal. There is also interatrial septal bowing towards the LA at end-systole. Of note, the linear dimensions and right atrial outline appear grossly smaller on the imaging screen than those from B), but this is because imaging depth is greater (notice the scale).

2. RVFWT (acute ≤ 5 mm, chronic > 5 mm) 3. TRPG (acute ≤ 46 mmHg, chronic > 46 mmHg; TRV_{max} ≤ 3.4 m/sec and > 3.4 m/sec, respectively) 4. PAAT (acute ≤ 60-80 msec, chronic < 105 msec) 5. 60/60 sign (acute) 6. PA ESN (proximally-located, higher-risk PE) 7. McConnell's sign (acute) 8. Right atrial enlargement (equal to left atrial size suggests acute, greater than left atrial size suggests chronic). By helping distinguish between acute and chronic right ventricular dysfunction, bedside echocardiography can lead to earlier goal-directed management.

A practical bedside algorithm for differentiating between acute and chronic right ventricular dysfunction begins by evaluating for the presence of a RHT. If there is none, determine the RVFWT. Next, search for TR and measure TRV_{max} for estimation of the TRPG. If no TR is visualized, generate the PA systolic ejection waveform to obtain PAAT and look for notching (none, early-, or mid-systolic). By having TRPG and PAAT, assess for the 60/60 sign. Finally, use McConnell's sign and the RA/LA size ratio only as supplemental adjuncts.

CRediT authorship contribution statement

Stephen Alerhand: Writing – review & editing, Writing – original draft, Visualization, Methodology, Conceptualization. **Robert James Adrian:** Writing – review & editing, Writing – original draft, Visualization, Methodology, Conceptualization.

Declaration of Competing Interest

None.

Supplementary data to this article can be found online at https://doi.org/10.1016/j.ajem.2023.07.011.

References

[1] Humbert M, Kovacs G, Hoeper MM, et al. 2022 ESC/ERS Guidelines for the diagnosis and treatment of pulmonary hypertension. Eur Respir J. 2023.;61(1).
[2] Alerhand S, Sundaram T, Gottlieb M. What are the echocardiographic findings of acute right ventricular strain that suggest pulmonary embolism? Anaesth Crit Care Pain Med. 2021;40(2):100852.
[3] Humbert M., Kovacs G., Hoeper M.M., et al. 2022 ESC/ERS Guidelines for the diagnosis and treatment of pulmonary hypertension. Eur Respir J. 2023 Jan 6;61(1): 2200879.
[4] The European Cooperative Study on the clinical significance of right heart thrombi. European Working Group on Echocardiography. Eur Heart J. 1989;10(12): 1046–59.
[5] Fields JM, Davis J, Girson L, et al. Transthoracic Echocardiography for Diagnosing Pulmonary Embolism: A Systematic Review and Meta-Analysis. J Am Soc Echocardiogr. 2017;30(7):714–723 e4.
[6] Falster C, Jacobsen N, Coman KE, et al. Diagnostic accuracy of focused deep venous, lung, cardiac and multiorgan ultrasound in suspected pulmonary embolism: a systematic review and meta-analysis. Thorax. 2022;77(7):679–89.
[7] Torbicki A, Galie N, Covezzoli A, et al. Right heart thrombi in pulmonary embolism: results from the International Cooperative Pulmonary Embolism Registry. J Am Coll Cardiol. 2003;41(12):2245–51.
[8] Casazza F, Becattini C, Guglielmelli E, et al. Prognostic significance of free-floating right heart thromboemboli in acute pulmonary embolism: results from the Italian Pulmonary Embolism Registry. Thromb Haemost. 2014;111(1):53–7.
[9] Barrios D, Rosa-Salazar V, Jimenez D, et al. Right heart thrombi in pulmonary embolism. Eur Respir J. 2016;48(5):1377–85.
[10] Kurnicka K, Lichodziejewska B, Goliszek S, et al. Echocardiographic Pattern of Acute Pulmonary Embolism: Analysis of 511 Consecutive Patients. J Am Soc Echocardiogr. 2016;29(9):907–13.
[11] Garvey S, Dudzinski DM, Giordano N, et al. Pulmonary embolism with clot in transit: An analysis of risk factors and outcomes. Thromb Res. 2020;187:139–47.
[12] Ibrahim WH, Ata F, Choudry H, et al. Prevalence, Outcome, and Optimal Management of Free-Floating Right Heart Thrombi in the Context of Pulmonary Embolism, a Systematic Review and Meta-Analysis. Clin Appl Thromb Hemost. 2022.;28 10760296221140114.
[13] Torbicki A, Perrier A, Konstantinides S, et al. Guidelines on the diagnosis and management of acute pulmonary embolism: the Task Force for the Diagnosis and Management of Acute Pulmonary Embolism of the European Society of Cardiology (ESC). Eur Heart J. 2008;29(18):2276–315.
[14] Casazza F, Bongarzoni A, Centonze F, et al. Prevalence and prognostic significance of right-sided cardiac mobile thrombi in acute massive pulmonary embolism. Am J Cardiol. 1997;79(10):1433–5.
[15] Habib G, Lancellotti P, Antunes MJ, et al. 2015 ESC Guidelines for the management of infective endocarditis: The Task Force for the Management of Infective Endocarditis of the European Society of Cardiology (ESC). Endorsed by: European Association for Cardio-Thoracic Surgery (EACTS), the European Association of Nuclear Medicine (EANM). Eur Heart J. 2015;36(44):3075–128.
[16] Silbiger JJ, Rashed E, Chen H, et al. Cardiac Imaging for Diagnosis and Management of Infective Endocarditis. J Am Soc Echocardiogr. 2022;35(9):910–24.
[17] Saric M, Armour AC, Arnaout MS, et al. Guidelines for the Use of Echocardiography in the Evaluation of a Cardiac Source of Embolism. J Am Soc Echocardiogr. 2016;29 (1):1–42.
[18] Habib G, Badano L, Tribouilloy C, et al. Recommendations for the practice of echocardiography in infective endocarditis. Eur J Echocardiogr. 2010;11(2):202–19.
[19] L'Angiocola PD, Donati R. Cardiac Masses in Echocardiography: A Pragmatic Review. J Cardiovasc Echogr. 2020;30(1):5–14.
[20] Peters PJ, Reinhardt S. The echocardiographic evaluation of intracardiac masses: a review. J Am Soc Echocardiogr. 2006;19(2):230–40.
[21] Moral S, Ballesteros E, Huguet M, et al. Differential Diagnosis and Clinical Implications of Remnants of the Right Valve of the Sinus Venosus. J Am Soc Echocardiogr. 2016;29(3):183–94.
[22] Howard LS, Grapsa J, Dawson D, et al. Echocardiographic assessment of pulmonary hypertension: standard operating procedure. Eur Respir Rev. 2012;21(125): 239–48.
[23] Dell'Italia LJ. Anatomy and physiology of the right ventricle. Cardiol Clin. 2012;30 (2):167–87.
[24] Friedberg MK, Redington AN. Right versus left ventricular failure: differences, similarities, and interactions. Circulation. 2014;129(9):1033–44.
[25] Pinsky MR. The right ventricle: interaction with the pulmonary circulation. Crit Care. 2016;20(1):266.
[26] van Wolferen SA, Marcus JT, Westerhof N, et al. Right coronary artery flow impairment in patients with pulmonary hypertension. Eur Heart J. 2008;29(1):120–7.
[27] Crystal GJ, Pagel PS. Right Ventricular Perfusion: Physiology and Clinical Implications. Anesthesiology. 2018;128(1):202–18.
[28] Moceri P, Baudouy D, Chiche O, et al. Imaging in pulmonary hypertension: Focus on the role of echocardiography. Arch Cardiovasc Dis. 2014;107(4):261–71.
[29] Vonk Noordegraaf A, Westerhof BE, Westerhof N. The Relationship Between the Right Ventricle and its Load in Pulmonary Hypertension. J Am Coll Cardiol. 2017; 69(2):236–43.

[30] Grapsa J, Dawson D, Nihoyannopoulos P. Assessment of right ventricular structure and function in pulmonary hypertension. J Cardiovasc Ultrasound. 2011;19(3):115–25.
[31] Rajiah P, MacNamara J, Chaturvedi A, et al. Bands in the Heart: Multimodality Imaging Review. Radiographics. 2019;39(5):1238–63.
[32] Vonk Noordegraaf A, Galie N. The role of the right ventricle in pulmonary arterial hypertension. Eur Respir Rev. 2011;20(122):243–53.
[33] Chin KM, Kim NH, Rubin LJ. The right ventricle in pulmonary hypertension. Coron Artery Dis. 2005;16(1):13–8.
[34] Bogaard HJ, Abe K, Vonk Noordegraaf A, et al. The right ventricle under pressure: cellular and molecular mechanisms of right-heart failure in pulmonary hypertension. Chest. 2009;135(3):794–804.
[35] Klima UP, Guerrero JL, Vlahakes GJ. Myocardial perfusion and right ventricular function. Ann Thorac Cardiovasc Surg. 1999;5(2):74–80.
[36] Lang RM, Badano LP, Mor-Avi V, et al. Recommendations for cardiac chamber quantification by echocardiography in adults: an update from the American Society of Echocardiography and the European Association of Cardiovascular Imaging. J Am Soc Echocardiogr. 2015;28(1):1–39 e14.
[37] Rudski LG, Lai WW, Afilalo J, et al. Guidelines for the echocardiographic assessment of the right heart in adults: a report from the American Society of Echocardiography endorsed by the European Association of Echocardiography, a registered branch of the European Society of Cardiology, and the Canadian Society of Echocardiography. J Am Soc Echocardiogr. 2010;23(7):685–713. quiz 786-8.
[38] Louridas G, Angomachalelis N, Patakas D, et al. Right ventricular echocardiographic, vectorcardiographic and electrocardiographic study in cor pulmonale. Acta Cardiol. 1980;35(6):429–36.
[39] Foale R, Nihoyannopoulos P, McKenna W, et al. Echocardiographic measurement of the normal adult right ventricle. Br Heart J. 1986;56(1):33–44.
[40] Matsukubo H, Matsuura T, Endo N, et al. Echocardiographic measurement of right ventricular wall thickness. A new application of subxiphoid echocardiography. Circulation. 1977;56(2):278–84.
[41] Ho SY, Nihoyannopoulos P. Anatomy, echocardiography, and normal right ventricular dimensions. Heart. 2006;92 Suppl 1(Suppl. 1):i2–13.
[42] You XD, Pu ZX, Peng XJ, et al. Tissue Doppler imaging study of right ventricular myocardial systolic activation in subjects with pulmonary arterial hypertension. Chin Med J (Engl). 2007;120(13):1172–5.
[43] Prakash R, Matsukubo H. Usefulness of echocardiographic right ventricular measurements in estimating right ventricular hypertrophy and right ventricular systolic pressure. Am J Cardiol. 1983;51(6):1036–40.
[44] Tsuda T, Sawayama T, Kawai N, et al. Echocardiographic measurement of right ventricular wall thickness in adults by anterior approach. Br Heart J. 1980;44(1):55–61.
[45] Prakash R. Echocardiographic diagnosis of right ventricular hypertrophy: correlation with ECG and necropsy findings in 248 patients. Cathet Cardiovasc Diagn. 1981;7(2):179–84.
[46] Prakash R. Reliability of echocardiography in the diagnosis of right ventricular hypertrophy. J Natl Med Assoc. 1982;74(8):767–71.
[47] Mumford M, Prakash R. Electrocardiographic and echocardiographic characteristics of long distance runners. Comparison of left ventricular function with age- and sex-matched controls. Am J Sports Med. 1981;9(1):23–8.
[48] Khemasuwan D, Yingchoncharoen T, Tunsupon P, et al. Right ventricular echocardiographic parameters are associated with mortality after acute pulmonary embolism. J Am Soc Echocardiogr. 2015;28(3):355–62.
[49] Park JH, Park MM, Farha S, et al. Impaired Global Right Ventricular Longitudinal Strain Predicts Long-Term Adverse Outcomes in Patients with Pulmonary Arterial Hypertension. J Cardiovasc Ultrasound. 2015;23(2):91–9.
[50] Ghio S, Pazzano AS, Klersy C, et al. Clinical and prognostic relevance of echocardiographic evaluation of right ventricular geometry in patients with idiopathic pulmonary arterial hypertension. Am J Cardiol. 2011;107(4):628–32.
[51] Cioffi G, de Simone G, Mureddu G, et al. Right atrial size and function in patients with pulmonary hypertension associated with disorders of respiratory system or hypoxemia. Eur J Echocardiogr. 2007;8(5):322–31.
[52] Kramer NE, Chawla KK, Patel R, et al. Differentiation of posterior myocardial infarction from right ventricular hypertrophy and normal anterior loop by echocardiography. Circulation. 1978;58(6):1057–64.
[53] Wilinski J, Skwarek A, Borek R, et al. Right ventricular wall thickness indexed to body surface area as an echocardiographic predictor of acute pulmonary embolism in high-risk patients. Kardiol Pol. 2022;80(2):205–7.
[54] D'Andrea A, La Gerche A, Golia E, et al. Right heart structural and functional remodeling in athletes. Echocardiography. 2015;32(Suppl. 1):S11–22.
[55] D'Andrea A, Morello A, Iacono AM, et al. Right Ventricular Changes in Highly Trained Athletes: Between Physiology and Pathophysiology. J Cardiovasc Echogr. 2015;25(4):97–102.
[56] Henriksen E, Kangro T, Jonason T, et al. An echocardiographic study of right ventricular adaptation to physical exercise in elite male orienteers. Clin Physiol. 1998;18(6):498–503.
[57] La Gerche A, Heidbuchel H, Burns AT, et al. Disproportionate exercise load and remodeling of the athlete's right ventricle. Med Sci Sports Exerc. 2011;43(6):974–81.
[58] Zoghbi WA, Adams D, Bonow RO, et al. Recommendations for Noninvasive Evaluation of Native Valvular Regurgitation: A Report from the American Society of Echocardiography Developed in Collaboration with the Society for Cardiovascular Magnetic Resonance. J Am Soc Echocardiogr. 2017;30(4):303–71.
[59] Spinner EM, Shannon P, Buice D, et al. In vitro characterization of the mechanisms responsible for functional tricuspid regurgitation. Circulation. 2011;124(8):920–9.
[60] Badano LP, Hahn R, Rodriguez-Zanella H, et al. Morphological Assessment of the Tricuspid Apparatus and Grading Regurgitation Severity in Patients With Functional Tricuspid Regurgitation: Thinking Outside the Box. JACC Cardiovasc Imaging. 2019;12(4):652–64.
[61] Hinderliter AL, Willis PWT, Long WA, et al. Frequency and severity of tricuspid regurgitation determined by Doppler echocardiography in primary pulmonary hypertension. Am J Cardiol. 2003;91(8):1033–7. A9.
[62] Lancellotti P, Moura L, Pierard LA, et al. European Association of Echocardiography recommendations for the assessment of valvular regurgitation. Part 2: mitral and tricuspid regurgitation (native valve disease). Eur J Echocardiogr. 2010;11(4):307–32.
[63] Yock PG, Popp RL. Noninvasive estimation of right ventricular systolic pressure by Doppler ultrasound in patients with tricuspid regurgitation. Circulation. 1984;70(4):657–62.
[64] McQuillan BM, Picard MH, Leavitt M, et al. Clinical correlates and reference intervals for pulmonary artery systolic pressure among echocardiographically normal subjects. Circulation. 2001;104(23):2797–802.
[65] Marra AM, Naeije R, Ferrara F, et al. Reference Ranges and Determinants of Tricuspid Regurgitation Velocity in Healthy Adults Assessed by Two-Dimensional Doppler-Echocardiography. Respiration. 2018;96(5):425–33.
[66] Torbicki A, Tramarin R, Morpurgo M. Role of echo/Doppler in the diagnosis of pulmonary embolism. Clin Cardiol. 1992;15(11):805–10.
[67] Kurzyna M, Torbicki A, Pruszczyk P, et al. Disturbed right ventricular ejection pattern as a new Doppler echocardiographic sign of acute pulmonary embolism. Am J Cardiol. 2002;90(5):507–11.
[68] Torbicki A, Kurzyna M, Ciurzynski M, et al. Proximal pulmonary emboli modify right ventricular ejection pattern. Eur Respir J. 1999;13(3):616–21.
[69] Augustine DX, Coates-Bradshaw LD, Willis J, et al. Echocardiographic assessment of pulmonary hypertension: a guideline protocol from the British Society of Echocardiography. Echo Res Pract. 2018;5(3):G11–24.
[70] Ciozda W, Kedan I, Kehl DW, et al. The efficacy of sonographic measurement of inferior vena cava diameter as an estimate of central venous pressure. Cardiovasc Ultrasound. 2016;14(1):33.
[71] Brennan JM, Blair JE, Goonewardena S, et al. Reappraisal of the use of inferior vena cava for estimating right atrial pressure. J Am Soc Echocardiogr. 2007;20(7):857–61.
[72] Finnerty NM, Panchal AR, Boulger C, et al. Inferior Vena Cava Measurement with Ultrasound: What Is the Best View and Best Mode? West J Emerg Med. 2017;18(3):496–501.
[73] Fields JM, Lee PA, Jenq KY, et al. The interrater reliability of inferior vena cava ultrasound by bedside clinician sonographers in emergency department patients. Acad Emerg Med. 2011;18(1):98–101.
[74] Zhou AZ, Green RS, Haines EJ, et al. Interobserver Agreement of Inferior Vena Cava Ultrasound Collapse Duration and Correlated Outcomes in Children With Dehydration. Pediatr Emerg Care. 2022;38(1):13–6.
[75] Akkaya A, Yesilaras M, Aksay E, et al. The interrater reliability of ultrasound imaging of the inferior vena cava performed by emergency residents. Am J Emerg Med. 2013;31(10):1509–11.
[76] D'Alto M, Bossone E, Opotowsky AR, et al. Strengths and weaknesses of echocardiography for the diagnosis of pulmonary hypertension. Int J Cardiol. 2018;263:177–83.
[77] Aslaner MA, Karbek Akarca F, Aksu SH, et al. Diagnostic Accuracy of Early Systolic Notching in Pulmonary Embolism. J Ultrasound Med. 2022;41(3):637–44.
[78] Terluk AD, Trivedi SJ, Kritharides L, et al. Echocardiographic Predictors of Long-Term Mortality in Patients Presenting With Acute Pulmonary Embolism. Am J Cardiol. 2019;124(2):285–91.
[79] Pruszczyk P, Goliszek S, Lichodziejewska B, et al. Prognostic value of echocardiography in normotensive patients with acute pulmonary embolism. JACC Cardiovasc Imaging. 2014;7(6):553–60.
[80] Pruszczyk P, Kurnicka K, Ciurzynski M, et al. Defining right ventricular dysfunction by echocardiography in normotensive patients with pulmonary embolism. Pol Arch Intern Med. 2020;130(9):741–7.
[81] Ciurzynski M, Kurnicka K, Lichodziejewska B, et al. Tricuspid Regurgitation Peak Gradient (TRPG)/Tricuspid Annulus Plane Systolic Excursion (TAPSE) - A Novel Parameter for Stepwise Echocardiographic Risk Stratification in Normotensive Patients With Acute Pulmonary Embolism. Circ J. 2018;82(4):1179–85.
[82] Afonso L, Sood A, Akintoye E, et al. A Doppler Echocardiographic Pulmonary Flow Marker of Massive or Submassive Acute Pulmonary Embolus. J Am Soc Echocardiogr. 2019;32(7):799–806.
[83] Ramberg E, Olausson M, Jorgensen TB, et al. Right atrial and ventricular function evaluated with speckle tracking in patients with acute pulmonary embolism. Am J Emerg Med. 2017;35(1):136–43.
[84] Bigdelu L, Daloee MH, Emadzadeh M, et al. Comparison of echocardiographic pulmonary flow Doppler markers in patients with massive or submassive acute pulmonary embolism and control group: A cross-sectional study. Health Sci Rep. 2023;6(5):e1249.
[85] D'Alto M, Di Maio M, Romeo E, et al. Echocardiographic probability of pulmonary hypertension: a validation study. Eur Respir J. 2022.;60(2).
[86] Murata M, Tsugu T, Kawakami T, et al. Prognostic value of three-dimensional echocardiographic right ventricular ejection fraction in patients with pulmonary arterial hypertension. Oncotarget. 2016;7(52):86781–90.
[87] Forfia PR, Fisher MR, Mathai SC, et al. Tricuspid annular displacement predicts survival in pulmonary hypertension. Am J Respir Crit Care Med. 2006;174(9):1034–41.
[88] Mouratoglou SA, Dimopoulos K, Kamperidis V, et al. Right Atrial Function Predicts Clinical Outcome in Patients with Precapillary Pulmonary Hypertension. J Am Soc Echocardiogr. 2018;31(10):1137–45.

[89] Burgess MI, Mogulkoc N, Bright-Thomas RJ, et al. Comparison of echocardiographic markers of right ventricular function in determining prognosis in chronic pulmonary disease. J Am Soc Echocardiogr. 2002;15(6):633–9.
[90] Aashish A, Giridharan S, Karthikeyan S, et al. Assessment of Pulmonary Artery Pressures by Various Doppler Echocardiographic Parameters and its Correlation with Cardiac Catheterization in Patients with Pulmonary Hypertension. Heart Views. 2020;21(4):263–8.
[91] Raymond RJ, Hinderliter AL, Willis PW, et al. Echocardiographic predictors of adverse outcomes in primary pulmonary hypertension. J Am Coll Cardiol. 2002;39 (7):1214–9.
[92] Mathai SC, Sibley CT, Forfia PR, et al. Tricuspid annular plane systolic excursion is a robust outcome measure in systemic sclerosis-associated pulmonary arterial hypertension. J Rheumatol. 2011;38(11):2410–8.
[93] Keir GJ, Wort SJ, Kokosi M, et al. Pulmonary hypertension in interstitial lung disease: Limitations of echocardiography compared to cardiac catheterization. Respirology. 2018;23(7):687–94.
[94] Amsallem M, Sternbach JM, Adigopula S, et al. Addressing the Controversy of Estimating Pulmonary Arterial Pressure by Echocardiography. J Am Soc Echocardiogr. 2016;29(2):93–102.
[95] Cordina RL, Playford D, Lang I, et al. State-of-the-Art Review: Echocardiography in Pulmonary Hypertension. Heart Lung Circ. 2019;28(9):1351–64.
[96] Dunham-Snary KJ, Wu D, Sykes EA, et al. Hypoxic Pulmonary Vasoconstriction: From Molecular Mechanisms to Medicine. Chest. 2017;151(1):181–92.
[97] Bossone E, Ferrara F, Grunig E. Echocardiography in pulmonary hypertension. Curr Opin Cardiol. 2015;30(6):574–86.
[98] Fisher MR, Forfia PR, Chamera E, et al. Accuracy of Doppler echocardiography in the hemodynamic assessment of pulmonary hypertension. Am J Respir Crit Care Med. 2009;179(7):615–21.
[99] Zaidi A, Knight DS, Augustine DX, et al. Echocardiographic assessment of the right heart in adults: a practical guideline from the British Society of Echocardiography. Echo Res Pract. 2020;7(1):G19–41.
[100] Bossone E, D'Andrea A, D'Alto M, et al. Echocardiography in pulmonary arterial hypertension: from diagnosis to prognosis. J Am Soc Echocardiogr. 2013;26(1):1–14.
[101] Brecker SJ, Gibbs JS, Fox KM, et al. Comparison of Doppler derived haemodynamic variables and simultaneous high fidelity pressure measurements in severe pulmonary hypertension. Br Heart J. 1994;72(4):384–9.
[102] Minagoe S, Rahimtoola SH, Chandraratna PA. Significance of laminar systolic regurgitant flow in patients with tricuspid regurgitation: a combined pulsed-wave, continuous-wave Doppler and two-dimensional echocardiographic study. Am Heart J. 1990;119(3 Pt 1):627–35.
[103] Fei B, Fan T, Zhao L, et al. Impact of severe tricuspid regurgitation on accuracy of systolic pulmonary arterial pressure measured by Doppler echocardiography: Analysis in an unselected patient population. Echocardiography. 2017;34(7): 1082–8.
[104] Giardini A, Tacy TA. Non-invasive estimation of pressure gradients in regurgitant jets: an overdue consideration. Eur J Echocardiogr. 2008;9(5):578–84.
[105] Wang YC, Huang CH, Tu YK. Pulmonary hypertension and pulmonary artery acceleration time: A systematic review and meta-analysis. J Am Soc Echocardiogr. 2018; 31(2):201–210 e3.
[106] Marra AM, Benjamin N, Ferrara F, et al. Reference ranges and determinants of right ventricle outflow tract acceleration time in healthy adults by two-dimensional echocardiography. Int J Cardiovasc Imaging. 2017;33(2):219–26.
[107] Weyman AE, Dillon JC, Feigenbaum H, et al. Echocardiographic patterns of pulmonic valve motion with pulmonary hypertension. Circulation. 1974;50(5): 905–10.
[108] Celermajer DS, Marwick T. Echocardiographic and right heart catheterization techniques in patients with pulmonary arterial hypertension. Int J Cardiol. 2008;125 (3):294–303.
[109] Yoshida T, Matsuura K, Seijirow G, et al. Non-invasive Assessment of Pulmonary Artery Wave Reflection in Dogs With Suspected Pulmonary Hypertension. Front Vet Sci. 2021;8:659194.
[110] Takahama H, McCully RB, Frantz RP, et al. Unraveling the RV Ejection Doppler Envelope: Insight Into Pulmonary Artery Hemodynamics and Disease Severity. JACC Cardiovasc Imaging. 2017;10(10 Pt B):1268–77.
[111] Kussmaul WG, Noordergraaf A, Laskey WK. Right ventricular-pulmonary arterial interactions. Ann Biomed Eng. 1992;20(1):63–80.
[112] Parker MW, Gottbrecht MF, Aurigemma GP. Midsystolic Notch and Pulmonary Hypertension: Pathophysiologic Mechanism and Technical Considerations. J Am Soc Echocardiogr. 2021;34(6):693–5.
[113] Bernard S, Namasivayam M, Dudzinski DM. Reflections on Echocardiography in Pulmonary Embolism-Literally and Figuratively. J Am Soc Echocardiogr. 2019;32 (7):807–10.
[114] Furuno Y, Nagamoto Y, Fujita M, et al. Reflection as a cause of mid-systolic deceleration of pulmonary flow wave in dogs with acute pulmonary hypertension: comparison of pulmonary artery constriction with pulmonary embolisation. Cardiovasc Res. 1991;25(2):118–24.
[115] Arkles JS, Opotowsky AR, Ojeda J, et al. Shape of the right ventricular Doppler envelope predicts hemodynamics and right heart function in pulmonary hypertension. Am J Respir Crit Care Med. 2011;183(2):268–76.
[116] Lopez-Candales A, Edelman K. Shape of the right ventricular outflow Doppler envelope and severity of pulmonary hypertension. Eur Heart J Cardiovasc Imaging. 2012;13(4):309–16.
[117] Naeije R, Huez S. Reflections on wave reflections in chronic thromboembolic pulmonary hypertension. Eur Heart J. 2007;28(7):785–7.
[118] Bech-Hanssen O, Lindgren F, Selimovic N, et al. Echocardiography can identify patients with increased pulmonary vascular resistance by assessing pressure reflection in the pulmonary circulation. Circ Cardiovasc Imaging. 2010;3(4):424–32.
[119] Castelain V, Herve P, Lecarpentier Y, et al. Pulmonary artery pulse pressure and wave reflection in chronic pulmonary thromboembolism and primary pulmonary hypertension. J Am Coll Cardiol. 2001;37(4):1085–92.
[120] Lodato JA, Ward RP, Lang RM. Echocardiographic predictors of pulmonary embolism in patients referred for helical CT. Echocardiography. 2008;25(6):584–90.
[121] Shah BR, Velamakanni SM, Patel A, et al. Analysis of the 60/60 Sign and Other Right Ventricular Parameters by 2D Transthoracic Echocardiography as Adjuncts to Diagnosis of Acute Pulmonary Embolism. Cureus. 2021;13(3):e13800.
[122] Shmueli H, Steinvil A, Aviram G, et al. Re-Appraisal of Echocardiographic Assessment in Patients with Pulmonary Embolism: Prospective Blinded Long-Term Follow-Up. Isr Med Assoc J. 2020;11(22):688–95.
[123] Zanobetti M, Converti C, Conti A, et al. Prognostic value of emergency physician performed echocardiography in patients with acute pulmonary thromboembolism. West J Emerg Med. 2013;14(5):509–17.
[124] Vitarelli A, Barilla F, Capotosto L, et al. Right ventricular function in acute pulmonary embolism: a combined assessment by three-dimensional and speckle-tracking echocardiography. J Am Soc Echocardiogr. 2014;27(3):329–38.
[125] Bustamante-Labarta M, Perrone S, De La Fuente RL, et al. Right atrial size and tricuspid regurgitation severity predict mortality or transplantation in primary pulmonary hypertension. J Am Soc Echocardiogr. 2002;15(10 Pt 2):1160–4.
[126] Vieillard-Baron A, Prin S, Chergui K, et al. Echo-Doppler demonstration of acute cor pulmonale at the bedside in the medical intensive care unit. Am J Respir Crit Care Med. 2002;166(10):1310–9.
[127] Martin-Duran R, Larman M, Trugeda A, et al. Comparison of Doppler-determined elevated pulmonary arterial pressure with pressure measured at cardiac catheterization. Am J Cardiol. 1986;57(10):859–63.
[128] Mazurek JA, Vaidya A, Mathai SC, et al. Follow-up tricuspid annular plane systolic excursion predicts survival in pulmonary arterial hypertension. Pulm Circ. 2017;7 (2):361–71.
[129] Burghuber OC, Brunner CH, Schenk P, et al. Pulsed Doppler echocardiography to assess pulmonary artery hypertension in chronic obstructive pulmonary disease. Monaldi Arch Chest Dis. 1993;48(2):121–5.
[130] Marchandise B, De Bruyne B, Delaunois L, et al. Noninvasive prediction of pulmonary hypertension in chronic obstructive pulmonary disease by Doppler echocardiography. Chest. 1987;91(3):361–5.
[131] Migueres M, Escamilla R, Coca F, et al. Pulsed Doppler echocardiography in the diagnosis of pulmonary hypertension in COPD. Chest. 1990;98(2):280–5.
[132] Gursel G, Ozdemir U, Guney T, et al. The usefulness of subxiphoid view in the evaluation of acceleration time and pulmonary hypertension in ICU patients. Echocardiography. 2020;37(9):1345–52.
[133] Tahara M, Tanaka H, Nakao S, et al. Hemodynamic determinants of pulmonary valve motion during systole in experimental pulmonary hypertension. Circulation. 1981;64(6):1249–55.
[134] Kitabatake A, Inoue M, Asao M, et al. Noninvasive evaluation of pulmonary hypertension by a pulsed Doppler technique. Circulation. 1983;68(2):302–9.
[135] Isobe M, Yazaki Y, Takaku F, et al. Prediction of pulmonary arterial pressure in adults by pulsed Doppler echocardiography. Am J Cardiol. 1986;57(4):316–21.
[136] Matsuda M, Sekiguchi T, Sugishita Y, et al. Reliability of non-invasive estimates of pulmonary hypertension by pulsed Doppler echocardiography. Br Heart J. 1986; 56(2):158–64.
[137] Ha B, Lucas CL, Henry GW, et al. Effects of chronically elevated pulmonary arterial pressure and flow on right ventricular afterload. Am J Physiol. 1994;267(1 Pt 2): H155–65.
[138] Turkevich D, Groves BM, Micco A, et al. Early partial systolic closure of the pulmonic valve relates to severity of pulmonary hypertension. Am Heart J. 1988;115 (2):409–18.
[139] Okamoto M, Miyatake K, Kinoshita N, et al. Analysis of blood flow in pulmonary hypertension with the pulsed Doppler flowmeter combined with cross sectional echocardiography. Br Heart J. 1984;51(4):407–15.
[140] Chiba Y, Iwano H, Murayama M, et al. Presence and relevance of midsystolic notching on right ventricular outflow tract flow velocity envelopes in pulmonary hypertension due to heart failure. J Am Soc Echocardiogr. 2021;34(6):690–692 e1.
[141] Burghuber OC. Doppler assessment of pulmonary haemodynamics in chronic hypoxic lung disease. Thorax. 1996;51(1):9–12.
[142] Laskey WK, Ferrari VA, Palevsky HI, et al. Pulmonary artery hemodynamics in primary pulmonary hypertension. J Am Coll Cardiol. 1993;21(2):406–12.
[143] Grant BJ, Lieber BB. Clinical significance of pulmonary arterial input impedance. Eur Respir J. 1996;9(11):2196–9.
[144] Naeije R, Torbicki A. More on the noninvasive diagnosis of pulmonary hypertension: Doppler echocardiography revisited. Eur Respir J. 1995;8(9):1445–9.
[145] Bergel DH, Milnor WR. Pulmonary Vascular Impedance in the Dog. Circ Res. 1965; 16:401–15.
[146] McConnell MV, Solomon SD, Rayan ME, et al. Regional right ventricular dysfunction detected by echocardiography in acute pulmonary embolism. Am J Cardiol. 1996; 78(4):469–73.
[147] Dwyer KH, Rempell JS, Stone MB. Diagnosing centrally located pulmonary embolisms in the emergency department using point-of-care ultrasound. Am J Emerg Med. 2018;36(7):1145–50.
[148] Eid M, Boghdady AM, Ahmed MM, et al. Echocardiographic findings in patients with acute pulmonary embolism at Sohag University Hospitals. Egypt J Intern Med. 2022;34(1):21.

[149] Daley JI, Dwyer KH, Grunwald Z, et al. Increased Sensitivity of Focused Cardiac Ultrasound for Pulmonary Embolism in Emergency Department Patients With Abnormal Vital Signs. Acad Emerg Med. 2019;26(11):1211–20.
[150] Lopez-Candales A, Edelman K. Right ventricular outflow tract systolic excursion: a distinguishing echocardiographic finding in acute pulmonary embolism. Echocardiography. 2013;30(6):649–57.
[151] Casazza F, Bongarzoni A, Capozi A, et al. Regional right ventricular dysfunction in acute pulmonary embolism and right ventricular infarction. Eur J Echocardiogr. 2005;6(1):11–4.
[152] Shah P, Schleifer JW, Mookadam F, et al. Right ventricular myocardial infarction: an underrecognized aetiology of McConnell's sign. Eur Heart J Cardiovasc Imaging. 2015;16(2):225.
[153] Longo SA, Echegaray A, Acosta CM, et al. McConnell's sign in intra-operative acute right ventricle ischaemia: An under-recognized aetiology. Rev Esp Anestesiol Reanim. 2016;63(9):528–32.
[154] Rafie N, Foley DA, Ripoll JG, et al. McConnell's sign is not always pulmonary embolism: the importance of right ventricular ischemia. JACC Case Rep. 2022;4(13):802–7.
[155] Gaynor SL, Maniar HS, Prasad SM, et al. Reservoir and conduit function of right atrium: impact on right ventricular filling and cardiac output. Am J Physiol Heart Circ Physiol. 2005;288(5):H2140–5.
[156] Gaynor SL, Maniar HS, Bloch JB, et al. Right atrial and ventricular adaptation to chronic right ventricular pressure overload. Circulation. 2005;112(9 Suppl):I212–8.
[157] Suga H. Importance of atrial compliance in cardiac performance. Circ Res. 1974;35(1):39–43.
[158] de Vroomen M, Cardozo RH, Steendijk P, et al. Improved contractile performance of right ventricle in response to increased RV afterload in newborn lamb. Am J Physiol Heart Circ Physiol. 2000;278(1):H100–5.
[159] Hon JK, Steendijk P, Khan H, et al. Acute effects of pulmonary artery banding in sheep on right ventricle pressure-volume relations: relevance to the arterial switch operation. Acta Physiol Scand. 2001;172(2):97–106.
[160] Willens HJ, Fertel DP, Qin J, et al. Effects of age and pulmonary arterial hypertension on the different phases of right atrial function. Int J Cardiovasc Imaging. 2008;24(7):703–10.
[161] Meng X, Li Y, Li H, et al. Right atrial function in patients with pulmonary hypertension: A study with two-dimensional speckle-tracking echocardiography. Int J Cardiol. 2018;255:200–5.
[162] Querejeta Roca G, Campbell P, Claggett B, et al. Right Atrial Function in Pulmonary Arterial Hypertension. Circ Cardiovasc Imaging. 2015;8(11):e003521. discussion e003521.
[163] Spencer KT, Garcia MJ, Weinart L, et al. Assessment of Right Ventricular and Right Atrial Systolic and Diastolic Performance Using Automated Border Detection. Echocardiography. 1999;16(7, Pt 1):643–52.
[164] D'Alto M, Scognamiglio G, Dimopoulos K, et al. Right heart and pulmonary vessels structure and function. Echocardiography. 2015;32(Suppl. 1):S3–10.
[165] Khan UA, Aurigemma GP, Tighe DA. Vector velocity imaging echocardiography to study the effects of submassive pulmonary embolism on the right atrium. Echocardiography. 2018;35(2):204–10.
[166] Sivak JA, Raina A, Forfia PR. Assessment of the physiologic contribution of right atrial function to total right heart function in patients with and without pulmonary arterial hypertension. Pulm Circ. 2016;6(3):322–8.
[167] Austin C, Alassas K, Burger C, et al. Echocardiographic assessment of estimated right atrial pressure and size predicts mortality in pulmonary arterial hypertension. Chest. 2015;147(1):198–208.
[168] Fukuda Y, Tanaka H, Motoji Y, et al. Utility of combining assessment of right ventricular function and right atrial remodeling as a prognostic factor for patients with pulmonary hypertension. Int J Cardiovasc Imaging. 2014;30(7):1269–77.
[169] Kou S, Caballero L, Dulgheru R, et al. Echocardiographic reference ranges for normal cardiac chamber size: results from the NORRE study. Eur Heart J Cardiovasc Imaging. 2014;15(6):680–90.
[170] Wang Y, Gutman JM, Heilbron D, et al. Atrial volume in a normal adult population by two-dimensional echocardiography. Chest. 1984;86(4):595–601.
[171] Whitlock M, Garg A, Gelow J, et al. Comparison of left and right atrial volume by echocardiography versus cardiac magnetic resonance imaging using the area-length method. Am J Cardiol. 2010;106(9):1345–50.
[172] Chow V, Ng AC, Chung T, et al. Right atrial to left atrial area ratio on early echocardiography predicts long-term survival after acute pulmonary embolism. Cardiovasc Ultrasound. 2013;11:17.
[173] Klasnja S, Manojlovic A, Popadic V, et al. Point-of-Care Echocardiographic Characteristics of COVID-19 Patients with Pulmonary Embolism. Diagnostics (Basel). 2022.;12(10).
[174] Siddiqui I, Rajagopal S, Brucker A, et al. Clinical and Echocardiographic Predictors of Outcomes in Patients With Pulmonary Hypertension. Am J Cardiol. 2018;122(5):872–8.
[175] Badagliacca R, Papa S, Valli G, et al. Echocardiography combined with cardiopulmonary exercise testing for the prediction of outcome in idiopathic pulmonary arterial hypertension. Chest. 2016;150(6):1313–22.